

Femtosecond Spectroscopic Studies of the One- and Two-Photon Excited-State Dynamics of 2,2,17,17-Tetramethyloctadeca-5,9,13-trien-3,7,11,15-tetrayne: A Trimeric Oligodiacylene

Grzegorz M. Balkowski,[†] Michiel Groeneveld,[†] Hong Zhang,^{*,†} Cindy C. J. Hendrikx,[‡] Michael Polhuis,[‡] Han Zuilhof,[‡] and Wybren J. Buma^{*,†}

Van't Hoff Institute for Molecular Sciences, University of Amsterdam, Nieuwe Achtergracht 166, 1018 WV Amsterdam, The Netherlands, and Laboratory of Organic Chemistry, Wageningen University, Dreijenplein 8, 6703 HA Wageningen, The Netherlands

Received: June 7, 2006; In Final Form: August 4, 2006

The excited-state dynamics of an oligomer of polydiacetylene, 2,2,17,17-tetramethyloctadeca-5,9,13-trien-3,7,11,15-tetrayne, dissolved in *n*-hexane have been studied by femtosecond fluorescence upconversion and polarized transient absorption experiments under one- and two-photon excitation conditions. Spectroscopically monitoring the population relaxation in the excited states in real time results in a distinct time separation of the dynamics. It has been concluded that the observed dynamics can be fully accounted for on the basis of the two lower excited states of the target molecule. The S_1 (2^1A_g) state, which cannot be excited from the ground state with one-photon absorption, is verified to be populated via internal conversion in 200 ± 40 fs from the strong dipole-allowed S_2 (1^1B_u) state. The population in the “hot” S_1 state subsequently cools with a time constant of 6 ± 1 ps and decays back to the ground state with a lifetime of 790 ± 12 ps.

I. Introduction

Because of their optoelectronic characteristics, molecules with extensive π conjugation are considered as high-potential candidates for applications such as field-effect transistors (FETs),^{1–3} light-emitting diodes (LEDs),^{4,5} and other devices.^{6,7} Polydiacetylenes (PDAs) form in this respect a unique class of materials that couple conjugated backbones with tailorable pendant side groups and terminal functionalities and exhibit dramatic chromogenic transitions that can be activated optically, thermally, chemically, and mechanically.^{8–11} The optoelectronic application of PDAs^{8,12,13} is related to their high nonlinearities^{14,15} and conducting properties.¹⁶ PDAs have been studied extensively over the years, as evidenced, for example, by a recent review.¹⁷ It is therefore even more remarkable that—despite the very large attention this class of polymers has received—still very basic questions remain on the nature and dynamics of their lower-lying electronically excited states. In view of the role of such states in optoelectronic applications, studies addressing such questions would be most welcome.

In the present study we have chosen to approach this subject not from the polymer side but study instead the lower-lying excited states of well-defined subunits of PDAs, oligodiacylenes, and, in particular, the trimeric unit 2,2,17,17-tetramethyloctadeca-5,9,13-trien-3,7,11,15-tetrayne (Figure 1), henceforth indicated as ODA3. This molecule has in the past already been subject to some experimental and theoretical spectroscopic studies. One- and two-photon fluorescence excitation studies at low temperatures¹⁸ showed convincingly that the lowest excited singlet state S_1 is not the strongly allowed 1^1B_u state, described in zero-order by the one-electron highest-occupied molecular orbital—lowest-unoccupied molecular orbital excita-

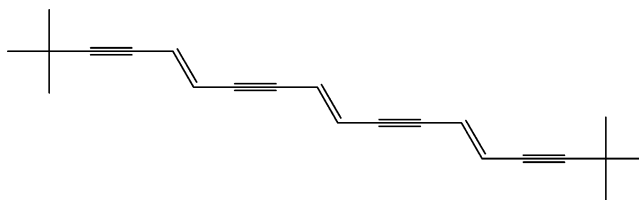


Figure 1. Structure of ODA3.

tion, but should instead be assigned to the strongly correlated 2^1A_g state that has significant double excitation character. The energy gap between the two states was found to be ~ 1700 cm^{-1} , which was somewhat larger than the gap between presumably analogous *ungerade* and *gerade* states determined from the frequency dependency of third harmonic generation in Langmuir–Blodgett films of PDAs.¹⁹ The assignment of Kohler and Schilke¹⁸ received further support from a theoretical study²⁰ that was capable to simulate the vibrational structure in the experimental absorption and emission spectra assuming that the absorption spectrum is associated with the S_2 (1^1B_u) \leftarrow S_0 (1^1A_g) transition and the emission spectrum with the S_1 (2^1A_g) \rightarrow S_0 (1^1A_g) transition. The same study showed that in the 1^1B_u state the electronic excitation is more or less localized on the center of the chain while in the 2^1A_g state the excitation is delocalized over all three butadienic fragments.

Recently, the spectroscopic properties of ODA3 have been investigated at room temperature in various solvents and incorporated into polymer films as part of a study to elucidate the effects of substituents and extended conjugation on the absorption and emission behavior.²¹ In this study the same conclusions on the identity of absorbing and emitting states were reached. Although the lifetime of the emissive state could be determined using time-correlated single photon counting techniques, the study could not observe the primary dynamic process(es) that happen directly after excitation of S_2 . In the present study we aim to elucidate precisely these processes. To this purpose we have employed femtosecond fluorescence

* To whom correspondence should be addressed. E-mail: h.zhang@uva.nl (H.Z.), w.j.buma@uva.nl (W.J.B.).

[†] University of Amsterdam.

[‡] Wageningen University.

upconversion and transient absorption techniques, in combination with studies of the decay of the polarization anisotropy. The comparison of these results with those of additionally performed two-photon excitation studies have enabled us to obtain a comprehensive view on the dynamics of the relevant excited states of ODA3.

II. Experimental Details

The synthesis of ODA3 has been reported elsewhere.²² ODA3 was dissolved in *n*-hexane (spectroscopic grade) purchased from Aldrich and used without further purification. Steady-state absorption and emission spectra were recorded on a Cary 3 (Varian) and Spex Fluorolog 3 spectrometer, respectively.

The femtosecond transient absorption setup has been described in detail previously.²³ Briefly, a ~ 100 fs (fwhm) pulse train at 800 nm with a repetition rate of 1 kHz is generated by a regenerative amplifier (Spectra Physics Hurricane). The pulse train is separated into two parts. One part is employed to pump a Spectra Physics OPA 800 that provides the excitation pulses—in the present case at 350 or 380 nm in one-photon experiments and 760 nm in two-photon experiments. The other part is focused on a calcium fluoride crystal to generate a white light continuum from ca. 350 to 800 nm that is used as the probe pulse. The total instrumental response is about 200 fs (fwhm). Unless stated otherwise, the time-resolved experiments were performed under magic-angle conditions and at ambient temperature on solutions with an optical density of ca. 1.0 in a 2-mm quartz cuvette. To avoid effects resulting from the high transient power radiation, the excitation power was kept as low as ~ 5 μ J per pulse with a spot area of ca. 0.5 mm². The influence of possible photodegradation of the sample was taken care of by stirring the solution as well. Absorption and emission spectra taken before and after time-resolved experiments were indeed identical, also in the case of the two-photon experiments in which the excitation energy was much higher.

The femtosecond fluorescence upconversion setup has been described in detail previously as well.²⁴ Briefly, 500- μ J laser pulses (~ 100 fs) at 800 nm with a repetition rate of 1 kHz were split into two beams. The main beam, with 90% of the total energy, serves to pump an optical parametric amplifier system (TOPAS Light Conversion Ltd.) that provides wavelength-tunable pulses from 310 to 390 nm to excite the sample, the other (weaker) beam serves as the gating beam for the detection. The fluorescence emitted from the sample is focused together with the gating beam on a 1 mm thick BBO crystal under type I phase-matching conditions. The generated upconversion signal is filtered by an UG 11 filter, focused onto the entrance slit of a monochromator, and detected using a photomultiplier that was connected to a lock-in amplifier system. The instrumental response time as determined by the cross-correlation signal of the excitation and gating pulses is approximately 280 fs (fwhm). Experiments have been performed under magic-angle conditions for pump and gating beams on solutions in a quartz cell of 1 mm thickness. The cell was attached to a sample holder that was moving perpendicularly to the excitation beam to prevent possible heating of the sample.

III. Results and Discussion

The steady-state absorption and emission spectra of ODA3 dissolved in *n*-hexane are depicted in Figure 2. The absorption spectrum shows two bands in the 200–400-nm region. A weaker band is located at 240 nm, while a stronger absorption occurs between 300 and 400 nm where a band with two sharp maxima at 350 and 380 nm is observed. Previous steady-state experiments performed at 77 K in 3-methylpentane¹⁸ and at room

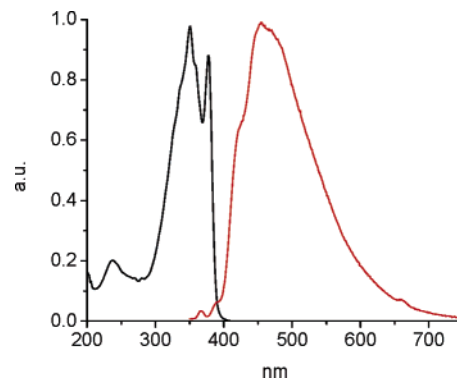


Figure 2. Steady-state absorption and emission spectra of ODA3 in *n*-hexane.

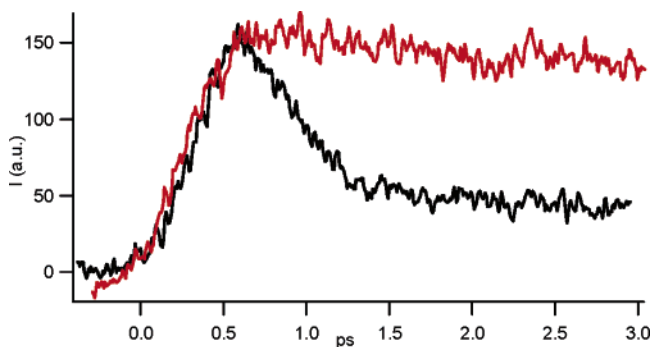


Figure 3. Fluorescence up-conversion transients of ODA3 dissolved in *n*-hexane. Excitation is at 350 nm. The black and red traces have been obtained for emission wavelengths of 454 and 533 nm, respectively.

temperature in *n*-hexane²¹ associate this band with the strongly allowed absorption to the lowest singlet state of *u* symmetry (1^1B_u). The emission spectrum has its maximum at about 455 nm with possibly unresolved shoulders around 425 and 465 nm. This is consistent with previous observations.^{18,21}

Fluorescence upconversion transients observed after one-photon excitation at 350 nm—the maximum of the absorption spectrum—have been recorded at various wavelengths as illustrated in Figure 3. At all detection wavelengths the signal contains two components—one being ultrafast (decay of 200 ± 40 fs), the other relatively slow (ca. 6 ps)—with relative contributions that are strongly wavelength dependent. On the blue side of the emission band, e.g., 454 nm, the decay is dominated by the ultrafast component. However, the contribution of this ultrafast component decreases significantly when the detection wavelength shifts to the red part of the emission band as illustrated by the transient observed at 533 nm where only the slow component appears.

We assign the observed ~ 200 fs decay to the internal conversion process from S_2 to S_1 . Emission from S_2 occurs at slightly higher energies than emission from S_1 . This implies that the shorter the detection wavelength in the fluorescence upconversion experiments, the larger the contribution of the $S_2 \rightarrow S_0$ transition is expected, and thus a more apparent ~ 200 fs decay component in the overall decay. On the other hand, increasing the detection wavelength should result in a smaller contribution from the $S_2 \rightarrow S_0$ transition, up to the point that for detection wavelengths larger than 530 nm the emission is only associated with the $S_1 \rightarrow S_0$ transition. For those wavelengths the signal is expected to show an in-growth with a time constant of 200 ± 40 fs. Indeed, the relative amplitude of the decaying component has been found to decrease with increasing detection wavelength, but a rise component has not been observed. We

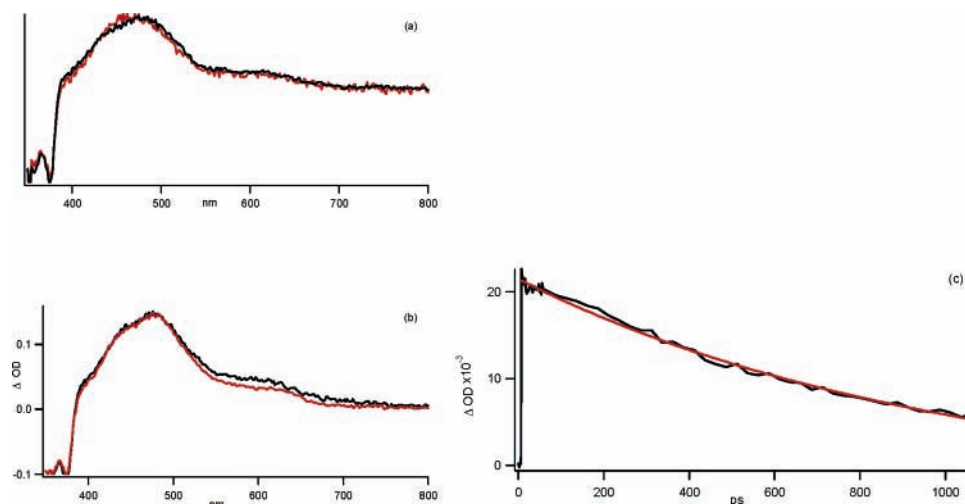


Figure 4. (a) Scaled transient absorption spectra of ODA3 in *n*-hexane taken at 20 ps (black) and 1000 ps (red) showing the absence of spectral evolution in this time period. (b) Scaled transient absorption spectra at 2 ps (black) and 40 ps (red) showing vibrational cooling in S_1 . (c) Observed (black) transient absorption decay at 470 nm. The red line is a monoexponential fit to this decay with a time constant of 790 ± 12 ps.

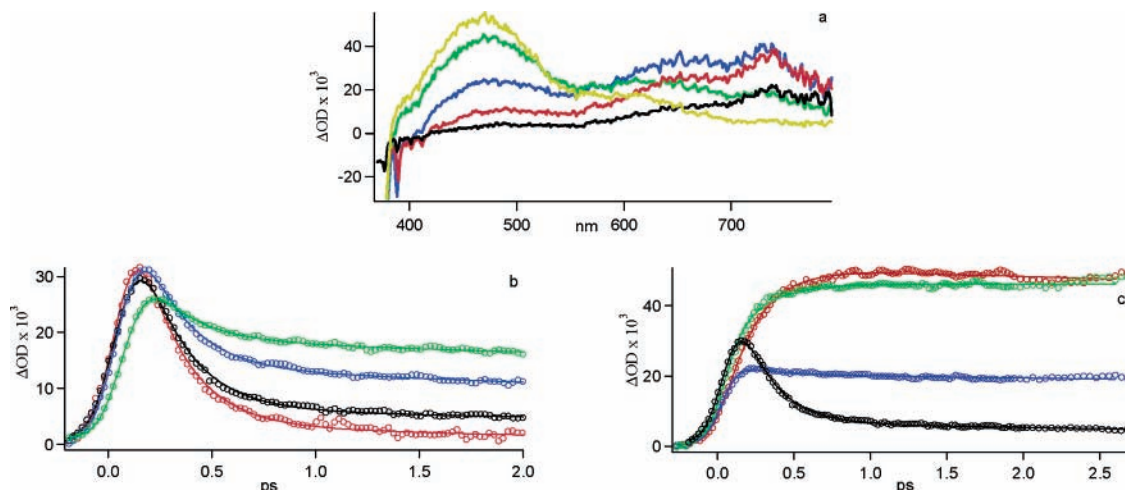


Figure 5. (a) Transient absorption spectrum at -200 (black), -100 (red), 0 (blue), 200 (green), and 800 (yellow) fs. (b) Transients in the red transient absorption bands at 600 (green), 650 (blue), 700 (black), and 750 (red) nm. (c) Transients in the blue transient absorption band at 550 (blue), 500 (green), and 450 (red) nm. For comparison the transient at 700 (black) nm is shown as well. The solid lines in parts b and c are fits to a triexponential function $\sum_{i=1,3} a_i \exp(-t/\tau_i)$ with $\tau_1 = 200$ fs, $\tau_2 = 6$ ps, and $\tau_3 = 790$ ps convoluted with the instrumental response.

attribute this to the fact that fluorescence upconversion was only possible near the maximum of the emission. The red tail of the emission, where the pure S_1 emission is located and the rise should be the most apparent, could not be detected due to its weakness. The transient absorption results to be discussed further on confirm this explanation.

A complementary view of the excited-state dynamics in ODA3 is provided by transient absorption experiments. In these experiments one-photon excitation wavelengths of 350 or 380 nm have been used. Since no differences could be observed between the transients obtained at these two wavelengths, we will in the following merely present and discuss the results obtained for excitation at 350 nm. The dynamics are observed to cover the time range from hundreds of femtoseconds to one nanosecond. For clarity we will therefore show the results in two separate time windows, a long time window of about 1 nanosecond (Figure 4) and a short time window that covers the first 10 picoseconds after photoexcitation and that has been recorded with a time step of 20 fs (Figure 5).

The transient absorption spectrum taken 20 ps after photoexcitation at 350 nm is shown in the black trace of Figure 4a. Comparison with the transient absorption spectrum obtained for a delay of 1 ns (red trace in Figure 4a) shows that the shape of

the spectrum basically remains the same and thus that after about 20 ps no evolution of the spectrum occurs. On this time scale, as illustrated in Figure 4c, decay traces at all wavelengths can be satisfactorily fitted with a monoexponential function with a decay time of 790 ± 12 ps. This decay time matches very well the fluorescence lifetime of ODA3 in *n*-hexane reported previously and is ascribed to the lifetime of the equilibrated S_1 state.²¹ From these results we can thus conclude that the excited-state absorption spectrum of S_1 of ODA3 shows two absorption bands in the 350–750 nm region: a strong band at 471 nm and a weaker one at 613 nm.

More complicated dynamics are revealed when the evolution of the absorption spectrum within the first picoseconds after excitation is considered. Transient absorption spectra collected at different delay times within the first picosecond are shown in Figure 5a. In the spectrum taken at a pump–probe delay of -200 fs, absorption bands appear with maxima at about 475, 650, and 720 nm, respectively, together with a ground-state bleaching signal below 400 nm. The intensity of the transient absorption increases with time and reaches a maximum at 0 fs for the 650- and 720-nm bands and 800 fs for the 475-nm band. The sharp, negative peak at ~ 390 nm visible in some of these spectra is attributed to Raman scattering of the solvent. Another

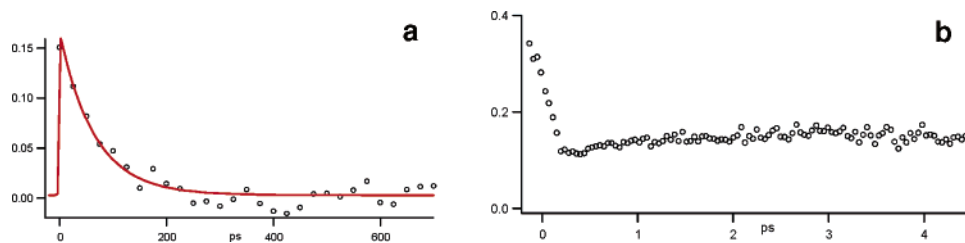


Figure 6. (a) Anisotropy decay of the transient absorption of the blue (~ 450 nm) band. Experimental data are indicated as circles, the drawn line is a monoexponential fit to these data with a time constant of 90 ± 5 ps. (b) Anisotropy decay of the transient absorption at 650 nm.

view on these ultrafast dynamics is provided by the transients obtained at 600, 650, 700, and 750 nm depicted in Figure 5b. All these transients exhibit an ultrafast component with a decay time of 200 ± 40 fs, but its relative amplitude is strongly wavelength dependent; for longer detection wavelengths its contribution increases. Transients obtained at the shorter wavelength band of the spectrum are given in Figure 5c for detection wavelengths of 550, 500, and 450 nm. These transients show evidence of the ultrafast component as well, which manifests itself now as an in-growth of the signal. In particular, the transient at 450 nm—where the contribution from absorption from the S_2 state is relatively small—shows a clear rise of the transient absorption from S_1 .

The fluorescence upconversion experiments have shown that after excitation of S_2 an ultrafast internal conversion process to S_1 occurs. In the transient absorption experiments, a ~ 200 -fs process is observed as well. Relating the changes in the transient absorption spectrum that occur on this time scale to this internal conversion process then leads to the conclusion that the absorptions at 650 and 720 nm are associated with excited-state absorption from the S_2 state and confirm our previous conclusion that the band at 475 nm derives from S_1 excited-state absorption. The $S_2 \rightarrow S_1$ internal conversion process can thus be directly traced in parts b and c of Figure 5, where the ~ 200 -fs ultrafast decay appears in the 700- and 750-nm traces and a corresponding rise is visible in the traces related to the 475-nm band. For some organic dyes, e.g., Nile Blue, Cresyl Violet, oxazine, and rhodamine compounds,^{25,26} it has been proposed that intramolecular redistribution of energy is responsible for the dynamics occurring on the time scale of several hundred femtoseconds. The rise of the 475-nm band and the concurrent decay of the 650- and 720-nm bands are clearly not compatible with such a scenario.

Figure 5c shows that the 475-nm band is subject to another dynamic process occurring in the picosecond time regime. This is most clear from the transients at 550 and 500 nm that display on this time scale an exponential decay and corresponding rise, respectively. The more subtle details of the spectral evolution that occurs on this time scale of a few picoseconds become clear from Figure 4b. Here it is observed that the blue side of the spectrum ($\lambda < 470$ nm) does not change from 2 to 40 ps, while the red shoulder from 550 to 700 nm narrows with time in the same time period. Fitting such transients reveals that the time constant associated with this process is 6 ± 1 ps. In view of the fact that it is the long wavelength side of the spectrum that narrows during this process, we assign this component to vibrational cooling in the S_1 state. Such processes have been the topic of a large number of studies on solvated organic molecules.^{27–30}

The polarization dependence of the transient absorption signals of ODA3 in *n*-hexane was studied by recording spectra for parallel and perpendicular configurations of the pump and probe beams. In these experiments it was found that for probe wavelengths in the blue absorption band around 475 nm the anisotropy has an initial value r_0 between 0.13 and 0.15 and a

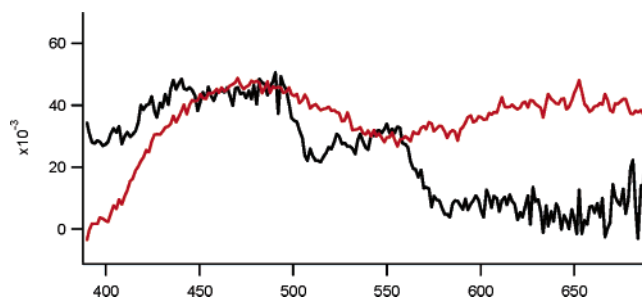


Figure 7. The absorption spectrum under two-photon excitation at 760 nm (black) at a pump-probe delay of 160 fs. The spectrum obtained for the same delay under one-photon excitation conditions at 380 nm is shown in red.

decay that can be fitted satisfactorily with a monoexponential function, yielding a depolarization time constant of 90 ± 5 ps (Figure 6a). In the previous time-correlated single-photon counting measurements significantly longer decay times were found. We attribute the observed differences to the higher laser powers employed in the present experiments, which will inevitably lead to local heating of the solution, and thus to a shortening of the rotational diffusion time. A completely different picture is obtained for the red band (Figure 6b). Here r_0 is roughly twice as large (0.34) and the anisotropy decays on a much faster time scale of ~ 200 fs. These observations are completely in line with the conclusions reached above on the $S_2 \rightarrow S_1$ internal conversion process and in fact provide further support for them. The initial anisotropy of 0.34 for the red band indicates that the transition moments of the $S_2 \leftarrow S_0$ and $S_n \leftarrow S_2$ transitions make an angle of about 18° and are thus reasonably parallel. Similarly we can conclude from the anisotropy of the blue band that the transition moments of the $S_2 \leftarrow S_0$ and $S_m \leftarrow S_1$ transitions are somewhat less parallel (41°), which comes as no surprise since completely different transitions are involved.

As yet, we have employed the one-photon strongly allowed 1^1B_u (S_2) state as our doorway state to enter the excited-state manifold of ODA3. Previous studies have established that the S_1 state is the 2^1A_g state.^{18,20} Excitation of this state is formally one-photon forbidden and only becomes partly allowed if the state would be vibronically coupled to a state of *u* symmetry. Under two-photon excitation conditions the 2^1A_g state becomes, however, fully allowed, while excitation of the 1^1B_u state is forbidden. It is therefore of interest to observe the transient absorption behavior of the molecule under such conditions, as it would confirm the ordering of states and possibly provide a different viewpoint on the excited-state dynamics. Figure 7 shows the transient absorption spectrum after two-photon excitation at 760 nm for a delay of 160 fs between pump and probe. Because of the high intensities employed for excitation, it was not possible to employ smaller delays. Although the signal-to-noise ratio in this spectrum is rather low, the comparison with the spectrum obtained with one-photon (380 nm) excitation at the same pump-probe delay shows distinct differences. In particular, we notice under two-photon excitation

conditions the absence of the bands in the 550–800-nm region that are clearly present using one-photon excitation. These results therefore confirm once more the presence of a state of different parity at lower excitation energies than the state that is responsible for the dominant absorption, and unambiguously demonstrate that two-photon excitation is able to populate exclusively the S_1 state without interference from the S_2 state.³¹ The presently employed two-photon excitation is also of interest to be employed to probe higher excitation energies. Here one might expect other *gerade* states such as the so-called m^1A_g state³² that cannot be observed in the steady-state absorption spectrum but are important for the nonlinear optical properties of this class of molecules.

The present study has shown that in ODA3 internal conversion from S_2 to S_1 occurs with a time constant of ~ 200 fs. It is interesting to notice that this decay time matches rather closely the lifetime of the photoexcited 1^1B_u free exciton in blue-phase PDAs, which was concluded to relax to the 2^1A_g exciton.³³ This might suggest that—as far as B_u internal conversion dynamics is concerned—ODA3 could be considered as a prototypical example for the longer chains in PDAs. We are presently investigating the validity of such a conclusion by studies of the dependence of the excited-state dynamics on the number of repeating enynic units in the oligodiacylene by similar studies as discussed here for the trimeric species on the monomeric, dimeric, and higher species up to $n = 8$.

The excited-state ordering and dynamics determined in the present study for ODA3 track very closely those observed for linear polyenes.^{34–37} For the smaller polyenes hexatriene and octatetraene it has been found that internal conversion from the S_2 to the S_1 state takes place with time constants of about 50 and 400 fs, respectively.^{38,39} It has been suggested that the large difference between the two could be attributed to a difference in S_2 – S_1 vibronic coupling strength and that internal conversion takes place along totally symmetric deformation coordinates.^{39,40} It would be interesting to study at a theoretical level whether the same mechanisms are responsible for the $S_2 \rightarrow S_1$ internal conversion in oligodiacylenes as well.

IV. Conclusions

Femtosecond fluorescence upconversion and transient absorption spectroscopic studies have been used to elucidate the energy relaxation mechanisms occurring after excitation of a prototypical polydiacylene oligomer ODA3 in a solution of *n*-hexane. The studies show that the primary deactivation channel of the one-photon strongly allowed 1^1B_u state is internal conversion to a lower-lying state occurring on a time scale of 200 ± 40 fs. On the basis of previous studies we associate this state with the 2^1A_g state. The same conclusion is reached from measurements of the decay of the polarization anisotropy of the various bands observed in the transient absorption spectrum. Upon internal conversion a “hot” S_1 state is created that is subject to vibrational cooling with a time constant of 6 ± 1 ps to reach the vibrationless S_1 state that has a lifetime of 790 ± 12 ps. Further support for the conclusion that internal conversion populates the 2^1A_g state has been obtained in transient absorption experiments with two-photon excitation that lead to the same transient absorption spectrum as observed after the internal conversion process following one-photon excitation. Since under two-photon excitation conditions the one-photon strongly allowed states are apparently invisible, this approach opens up the door to detailed studies of the excited-state dynamics of other, higher-lying *gerade* states.

Acknowledgment. This work was supported by The Netherlands Organization for Scientific Research (NWO). Financial

support from NOVEM and Wageningen University is gratefully acknowledged.

References and Notes

- Hong, X. M.; Katz, H. E.; Lovinger, A. J.; Wang, B. C.; Raghavachari, K. *Chem. Mater.* **2001**, *13*, 4686.
- Xu, G.; Bao, Z.; Groves, J. T. *Langmuir* **2000**, *16*, 1834.
- Katz, H. E.; Bao, Z. *J. Phys. Chem. B* **2000**, *104*, 671.
- Zheng, L.; Urian, R. C.; Liu, Y.; Jen, A. K.-Y.; Pu, L. *Chem. Mater.* **2000**, *12*, 13.
- Pei, J.; Yu, W.-L.; Ni, J.; Lai, Y.-H.; Haung, W.; Heeger, A. J. *Macromolecules* **2001**, *34*, 7241.
- Gan, H.; Liu, L.; H. Y.; Zhao, Q.; Li, Y.; Wang, S.; Jiu, T.; Wang, N.; He, X.; Yu, D.; Zhu, D. *J. Am. Chem. Soc.* **2005**, *127*, 12452.
- McQuade, D. T.; Pullen, A. E.; Swager, T. M.; *Chem. Rev.* **2000**, *100*, 2537.
- Carpick, R. W.; Sasaki, D. Y.; Marcus, M. S.; Eriksson, M. A.; Burns, A. R. *J. Phys. Condens. Matter* **2004**, *16*, 679.
- Jung, Y. K.; Park, H. G.; Kim, J. M. *Biosens. Bioelectron.* **2006**, *21*, 1536.
- S. J. Kew, E. A. H. Hall *Anal. Chem.* **2006**, *78*, 2231.
- Peng, H. S.; Tang, J.; Pang, J. B.; Chen, D. Y.; Yang, L.; Ashbaugh, H. S.; Brinker, C. J.; Yang, Z. Z.; Lu, Y. F. *J. Am. Chem. Soc.* **2005**, *127*, 12782.
- Kolusheva, S.; Molt, O.; Herm, M.; Schrader, T.; Jelinek, R. *J. Am. Chem. Soc.* **2005**, *127*, 10000.
- Pinzola, B. A.; Nguyen, A. T.; Reppy, M. A. *Chem. Commun.* **2006**, *28*, 906.
- Carter, G. M.; Thakur, M. K.; Chen, Y. J.; Hryniewicz, J. V. *Appl. Phys. Lett.* **1985**, *47*, 457.
- Rao, D. N.; Chopra, P.; Ghoshal, S. K.; Swiatkiewicz, J.; Prasad, P. N. *J. Chem. Phys.* **1986**, *84*, 7049.
- Takami, K.; Mizuno, J.; Akai-kasaya, M.; Saito, A.; Aono, M.; Kuwahara, Y. *J. Phys. Chem. B* **2004**, *108*, 16353.
- Zuilhof, H.; Barentsen, H. M.; Dijk, M. van; Südhöf, E. J. R.; Hoofman, R. J. O. M.; Siebbeles, L. D. A.; Haas, M. P. de; Warman, J. M. In *Supramolecular Photosensitive and Electroactive Materials*; Nalwa, H. S., Ed.; Academic Press: Los Angeles, 2001; pp 339–437.
- Kohler, B. E.; Schilke, D. E. *J. Chem. Phys.* **1987**, *86*, 5214.
- Kajzar, F.; Messier, J. *Thin Solid Films* **1985**, *132*, 11.
- Zerbetto, F. *J. Phys. Chem.* **1994**, *98*, 13157.
- Hendrikx, C. C. J.; Polhuis, M.; Pul-Hootsen, A.; Koehorst, R. B. M.; Hoek, A. van; Zuilhof, H.; Südhöf, E. J. R. *PCCP* **2005**, *7*, 548.
- Polhuis, M.; Hendrikx, C. C. J.; Zuilhof, H.; Südhöf, E. *Tetrahedron Lett.* **2003**, *44*, 899.
- Balkowski, G.; Szemik-Hojniak, A.; van Stokkum, I. H. M.; Zhang, H.; Buma, W. J. *J. Phys. Chem. A* **2005**, *109*, 3535.
- Humbs, W.; Zhang, H.; Glasbeek, M. *Chem. Phys.* **2000**, *254*, 319.
- Laermer, F.; Elsaesser, T.; Kaiser, W. *Chem. Phys. Lett.* **1989**, *156*, 4.
- Laermer, F.; Israel, W.; Elsaesser, T. *J. Opt. Soc. Am. B* **1990**, *7*, 1604.
- Seifert, G.; Patzlaff, T.; Paradowska-Moszkowska, K.; Graener, H. *Chem. Phys.* **2005**, *79*, 392.
- Chudoba, C.; Nibbering, E. T. J.; Elsaesser, T. *Phys. Rev. Lett.* **1998**, *81*, 3010.
- Horng, M. L.; Gardecki, J. A.; Papazyan, A.; Maroncelli, M. *J. Phys. Chem.* **1995**, *99*, 17311.
- Shank, C. V.; Ippen, E. P.; Teschke, O. *Chem. Phys. Lett.* **1977**, *45*, 291.
- Theoretically the one-photon allowed states might still be excited under two-photon excitation conditions if vibronic coupling with two-photon allowed states would be strong. In that case such states might still interfere in the two-photon absorption spectrum.
- Race, A.; Barford, W.; Bursill, R. *J. Phys. Rev. B* **2001**, *64*, 035208.
- Yoshizawa, M.; Kubo, A.; Saikan, S. *Phys. Rev. B* **1999**, *60*, 15632.
- Orlandi, G.; Zerbetto, F.; Zgierski, M. *Z. Chem. Rev.* **1991**, *91*, 867 and references therein.
- Buma, W. J.; Song, K.; Kohler, B. E. *J. Chem. Phys.* **1990**, *92*, 4622; *ibid.* **1991**, *94*, 6367.
- Buma, W. J.; Kohler, B. E.; Shaler, T. A. *J. Chem. Phys.* **1992**, *96*, 399.
- Petek, H.; Bell, A. J.; Choi, Y. S.; Yoshihara, K.; Tounge, B. A.; Christensen, R. L.; *J. Chem. Phys.* **1993**, *98*, 3777; *ibid.* **1995**, *102*, 4726.
- Anderson, N. A.; Durfee, C. G.; Murnane, M. M.; Kapteyn, H. C.; Sensen, R. *J. Chem. Phys. Lett.* **2000**, *323*, 365–371.
- Ohta, K.; Naitoh, Y.; Keisuke, T.; Yoshihara, K. *J. Phys. Chem. A* **2001**, *105*, 3973.
- Garavelli, M.; Celani, P.; Bernardi, F.; Robb, M. A.; Olivucci, M. *J. Am. Chem. Soc.* **1997**, *119*, 11487.